tvst

Retina

Postoperative Proliferation Detection in Eyes Treated for Rhegmatogenous Retinal Detachment by WideField OCT Angiography

Yosuke Fukuda[1], Keijiro Ishikawa[1], Kohei Kiyohara[1], Yusuke Maehara[1], Rui Ji[1], Kenichiro Mori[1], Yoshiyuki Kobayashi[1], Masato Akiyama[1], Takahito Nakama[1,2], Shoji Notomi[1], Satomi Shiose[1], Atsunobu Takeda[1], and Koh-Hei Sonoda[1]

[1] Department of Ophthalmology, Graduate School of Medical Sciences, Kyushu University, Fukuoka, Japan
[2] Department of Ophthalmology, Aso Iizuka Hospital, Fukuoka, Japan

Correspondence: Keijiro Ishikawa, Department of Ophthalmology, Graduate School of Medical Sciences, Kyushu University, 3-1-1 Maidashi, Higashi-Ku, Fukuoka 812-8582, Japan. e-mail: ishikawa.keijiro.609@m.kyushu-u.ac.jp

Received: April 26, 2024
Accepted: June 29, 2024
Published: August 8, 2024

Keywords: proliferative vitreoretinopathy; retinal thickness; retinal vessel tortuosity; rhegmatogenous retinal detachment (RRD); widefield OCT (WF-OCT); widefield OCT angiography (WF-OCTA)

Citation: Fukuda Y, Ishikawa K, Kiyohara K, Maehara Y, Ji R, Mori K, Kobayashi Y, Akiyama M, Nakama T, Notomi S, Shiose S, Takeda A, Sonoda KH. Postoperative proliferation detection in eyes treated for rhegmatogenous retinal detachment by widefield OCT angiography. Transl Vis Sci Technol. 2024;13(8):13, https://doi.org/10.1167/tvst.13.8.13

Purpose: Proliferative retinal changes may occur postsurgery for rhegmatogenous retinal detachment (RRD), possibly preceding recurrent detachment. This study aims to establish the groundwork for an imaging system capable of discerning changes in retinal vessel tortuosity after RRD repair, analyzing widefield optical coherence tomography angiography (WF-OCTA) images.

Methods: Eighty-eight eyes of 86 patients with RRD who underwent surgical procedures and had repeated imaging with clear widefield optical coherence tomography (WF-OCT) and WF-OCTA on different postoperative days were enrolled in this retrospective study. We compared WF-OCTA images over time to identify alterations in retinal vessel tortuosity and observed regional changes in retinal morphology.

Results: After image processing, changes in retinal vessel tortuosity were detected in 66 quadrants. These changes, attributed to retinal traction from proliferative membranes, were observed in 56 quadrants, among which retinal thickness remained unchanged in seven sectors (12.5%) according to the WF-OCT map. In nine quadrants, changes in retinal vessel tortuosity were attributed to changes in subretinal fluid, aligning with observable variations in retinal thickness.

Conclusions: Observation of vessel tortuosity changes using WF-OCTA can help detect early postoperative proliferative changes in eyes with RRD.

Translational Relevance: Because WF-OCTA can detect minute vessel tortuosity changes, it can offer a noninvasive alternative for the detection of early postoperative proliferative changes.

Introduction

Recent advancements in retinal detachment (RD) surgery have significantly improved success rates,[1] with over 90% of uncomplicated rhegmatogenous RD (RRD) cases reattached successfully in a single operation.[2,3] In addition, numerous recent reports on postoperative outcomes and changing surgical techniques underscore ongoing efforts to optimize methods.[4–9] However, proliferative vitreoretinopathy (PVR) remains a major RRD surgery complication

and the leading cause of surgical failure.[10] Unfortunately, no pharmacologic treatment for PVR exists, and surgical removal of proliferative membranes is the only effective treatment option.[10] PVR is characterized by excessive cell proliferation on the retinal surface or within the vitreous cavity, resulting in retinal traction and recurrent detachment.[11,12]

The pursuit of effective PVR prevention measures has prompted the extensive investigation of various pharmaceutical agents. However, the current state of drug discovery in this domain is generally perceived as insufficient, as highlighted in a previous study.[13] If a viable pharmaceutical intervention for PVR prevention is established, early recognition of PVR symptoms becomes of paramount importance. It has been postulated that the presence of minor vascular tortuosity can serve as an early indicator of impending PVR, as delineated by the aforementioned PVR grading system.[14]

Optical coherence tomography (OCT) and OCT angiography (OCTA) have become indispensable tools for assessing macular and vitreoretinal interface disorders. Importantly, widefield OCT (WF-OCT) and widefield OCTA (WF-OCTA) permit the exploration of peripheral retinal structures through B-scan and en face imaging techniques.[15,16] The Xephilio OCT-S1 (Canon, Tokyo, Japan), introduced in 2019, captures expansive B-scan images up to 23 mm. Moreover, it obtains WF-OCTA images (23 × 20 mm) in a single scan, harnessing artificial intelligence capabilities for high-resolution images.

The objective of this study is to use a combination of WF-OCT and WF-OCTA in conjunction with specialized imaging software to detect alterations in retinal vessel tortuosity in patients with PVR after surgical intervention for RRD repair.

Methods

Study Design

This retrospective case series, following the principles of the Declaration of Helsinki, was approved by the Institutional Review Board of Kyushu University. Written informed consent was obtained from all the patients, and data were anonymized before analysis.

This study included eyes with RRD that underwent vitreoretinal surgery at Kyushu University Hospital from March 2021 to October 2022. Before surgery, all patients underwent ophthalmic examinations, including WF fundus photography (Optos California, Optos Inc., Dunfermline, Scotland), WF-OCT, and WF-OCTA (Xephilio OCT-S1). Eyes with noisy WF-OCTA images and eyes in which RRD could be definitively attributed to trauma were excluded.

To ensure the reliability of detecting retinal vessel tortuosity changes and accuracy of alignment by the image processing used in this study, we also examined 48 healthy eyes, capturing WF-OCT and WF-OCTA images twice on the same day.

Evaluation of Retinal Vessel Tortuosity Changes by WF-OCTA

In this study, we obtained high-resolution WF-OCTA images of a 20-mm vertical (807 B-scans) and 23-mm horizontal (1024 pixels) retina. The entire retinal structure, from the inner limiting membrane (ILM) to the retinal pigment epithelium (RPE), was comprehensively imaged, and automatic segmentation was performed using integrated artificial intelligence software.

We acquired WF-OCTA images of eyes with postoperative RRD at two distinct time points: 1 and 2 months after surgery. For comparative analysis, we color-coded the 1-month and 2-month postoperative WF-OCTA images in red and green, respectively, using ImageJ (National Institutes of Health, Bethesda, MD, USA). These color-coded images were superimposed (Figs. 1A–E). To assess the alterations in retinal vessel tortuosity, we divided the superimposed WF-OCTA images into four quadrants: superior, temporal, inferior, and nasal. The observer viewed overlaid OCTA images while being blinded to patient information to ensure unbiased assessment. A change in retinal vessel tortuosity was defined as the displacement of retinal blood vessels by 10 pixels or more within each quadrant. However, this approach may be influenced by head misalignment and ocular rotation.

To mitigate these potential sources of error, we applied alignment procedures to the WF-OCTA images using the image software i2k Retina Pro (DualAlign, New York, NY, USA), which is capable of automated image alignment. This software algorithm identifies features in small portions of an input image and, in ophthalmic images, analyzes and compares the unique characteristics of vascular structures such as edges and branching points. In recent years, this software has been increasingly used to capture subtle changes in retinal vasculature on widefield images.[17,18] After alignment, we repeated the color-coding and superimposition process for the 1- and 2-month postoperative WF-OCTA images (Figs. 1F, 1J). These overlaid images were again divided into four quadrants, and the criteria for identifying changes in retinal vessel tortuosity remained consistent with the previous assessment. We

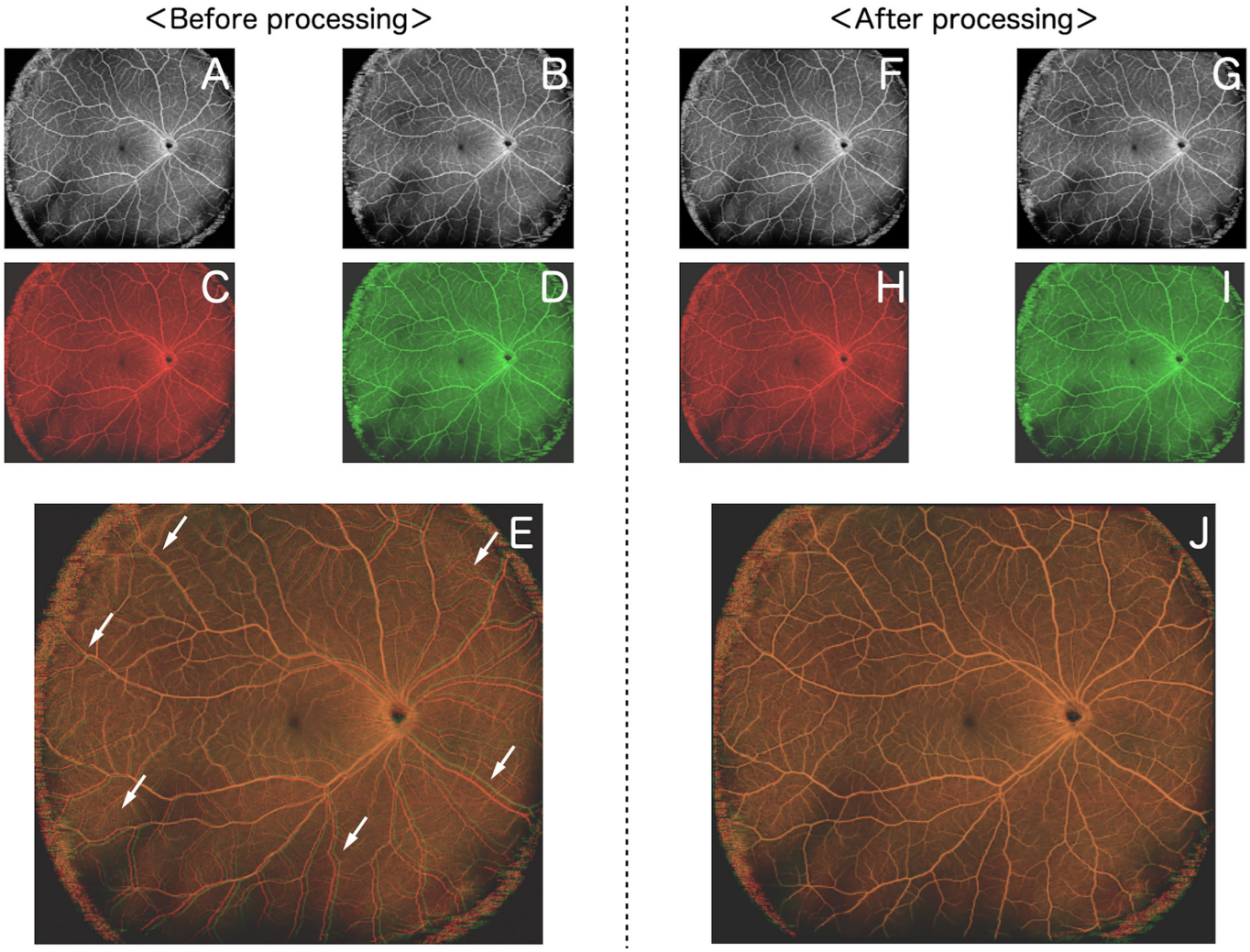

Figure 1. Overlay healthy eye images (before or after processing). Both **A** and **B** show OCTA images of healthy eyes obtained on the same day. The color of each image was changed to *red* (**C**) or *green* (**D**). After **C** and **D** are overlaid, the *white arrows* indicate that the retinal vessels do not overlap in all quadrants (**E**). **F** and **G** are obtained by processing **A** and **B** using image-processing software. The color of each image was changed to *red* (**H**) or *green* (**I**). After **H** and **I** are overlaid, the retinal vessels overlap exactly (**J**).

systematically investigated the causes of these alterations when detected, involving careful examination of WF-OCT B-scan images. We categorized the identified causes based on B-scan findings and meticulously documented the affected quadrants.

Evaluation of Retinal Thickness Changes by WF-OCT

In patients with RRD, three-dimensional volumetric data were obtained through WF-OCT. The data covered a 20-mm vertical and 23-mm horizontal region (1024 pixels) with a 5.3-mm scan depth. Retinal thickness was assessed by measuring the vertical distance between the ILM and RPE layers. Automated segmentation of these layers was performed using artificial intelligence–supported software.

We used the OCT Research Tool (Canon Medical Systems, Ōtawara, Japan) to identify retinal thickness changes. This tool facilitated comparison of retinal thickness maps and extraction of differential thickness data. The extracted images were subsequently divided into four quadrants, defining a change in retinal thickness as a variation of $\geq$30 µm within each quadrant.

Statistical Analysis

Data are presented as frequencies for categorical variables and as mean $\pm$ standard deviation. Differences between groups were assessed using Fisher's exact test for categorical variables and one-way analy-

sis of variance for continuous variables. $P < 0.05$ was considered significant.

Results

In this study, we examined 88 eyes of 86 patients with RRD. The study group, consisting of 60 men and 26 women, had an average age of 50.0 ± 16.7 years. Among these eyes, 56 underwent pars plana vitrectomy, 27 had scleral buckling, and 5 had a combination of both procedures.

In a cohort of 48 healthy eyes, we initially identified retinal vessel tortuosity changes in 65 of 192 quadrants (33.9%) before processing. Following processing with i2k Retina Pro, no such changes were observed (Table 1). Conversely, among the 88 eyes with RRD, we identified retinal vessel tortuosity changes in 309 of the 352 quadrants (87.8%) before processing. After processing, the number of quadrants showing these changes was reduced to 66 of 352 (18.8%) (Table 1).

Upon detailed B-scan image examination, we determined that retinal vessel tortuosity changes in RRD eyes could be attributed to increased retinal thickness by proliferative membranes (epiretinal membrane) or alterations in subretinal fluid. Specifically, 56 quadrants (84.8%) exhibited changes due to increased retinal traction by proliferative membranes, while 9 quadrants (13.6%) demonstrated changes due to alterations in subretinal fluid levels. Both factors were simultaneously implicated in a single quadrant (Table 2). Based on the reference to WF fundus photography and medical records, no new lesions affecting retinal vasculature were found between 1 and 2 months postsurgery. Therefore, it was considered that the causes of the retinal vessel tortuosity changes were likely due to proliferative membranes and alterations in subretinal fluid levels.

Table 1. Number of Quadrants Where Retinal Vessel Tortuosity Differences Were Detected Before and After Image Processing

Characteristic	*n* (%)
Healthy eyes (192 quadrants of 48 eyes)	
Before processing (quadrants)	65 (33.9)
After processing (quadrants)	0 (0)
RRD eyes (352 quadrants of 88 eyes)	
Before processing (quadrants)	309 (87.8)
After processing (quadrants)	66 (18.8)

Notably, in all nine quadrants where changes in retinal vessel tortuosity were attributed to variations in the subretinal fluid, corresponding retinal thickness changes were detected. In contrast, among the 56 quadrants where changes were caused by the exacerbation of retinal traction due to proliferative membranes, retinal thickness changes were not observed in seven quadrants (Table 2). We further explored the location where changes in retinal vessel tortuosity occurred and found a tendency for these changes to be more common in the temporal and inferior quadrants. This distribution remained consistent, regardless of the causative factors behind the retinal vessel tortuosity changes, and there were no significant differences.

This study specifically included cases with clear WF-OCTA images at both 1 and 2 months postoperatively and with no cases undergoing reoperation within 3 months postsurgery. We obtained OCTA images for all 88 eyes with RRD at 3 months postoperatively. Among the 66 quadrants where retinal vessel tortuosity changes occurred between 1 and 2 months postoperatively, 14 quadrants (21.2%) showed further progression between 2 and 3 months postoperatively. Interestingly, among the quadrants where retinal vessel tortuosity changes did not occur between 1 and 2 months postoperatively, no new occurrences of retinal vessel

Table 2. Morphologic Changes Evaluated in B-Scan Images Where Retinal Vessel Tortuosity Changes Were Detected on WF-OCTA and the Location of Retinal Vessel Tortuosity Changes

	Morphologic Changes in B-Scan Images, *n* (%)			
Characteristic	Proliferation ($n = 56$)	Subretinal Fluid ($n = 9$)	Both ($n = 1$)	Total ($N = 66$)
Detected by OCT map	49 (87.5)	9 (100)	1 (100)	59 (89.4)
Not detected by OCT map	7 (12.5)	0 (0)	0 (0)	7 (10.6)
Location*				
Superior	12 (21.4)	1 (11.1)	1 (100)	14 (21.2)
Temporal	17 (30.4)	3 (33.3)	0 (0)	20 (30.3)
Inferior	16 (28.6)	3 (33.3)	0 (0)	19 (28.8)
Nasal	11 (19.6)	2 (22.2)	0 (0)	13 (19.7)

*$P = 0.96$ (Fisher's exact test).

Table 3. Comparison of Study Subjects' Baseline Characteristics and Surgical Procedures in Vitrectomy

Characteristic	Proliferation ($n = 21$)	No Proliferation ($n = 40$)	*P* Value
Gender, *n* (%)			0.38
Male	13 (61.9)	30 (75.0)	
Female	8 (38.1)	10 (25.0)	
Age, mean ± SD, y	60.1 ± 11.4	55.7 ± 11.1	0.15
Axial length, mean ± SD, mm	25.5 ± 1.4	25.7 ± 1.7	0.69
BCVA, mean ± SD, logMAR	0.56 ± 0.59	0.55 ± 0.74	0.96
IOP, mean ± SD, mm Hg	14.8 ± 1.0	13.2 ± 0.8	0.22
Lens status, *n* (%)			0.21
Phakia	14 (66.7)	33 (82.5)	
Pseudophakia	7 (33.3)	7 (17.5)	
Macula status, *n* (%)			0.43
On	9 (42.9)	22 (55.0)	
Off	12 (57.1)	18 (45.0)	
RD area, mean ± SD, quadrants			0.03
1	3 (14.3)	17 (42.5)	
2	17 (80.9)	18 (45.0)	
3	1 (4.8)	4 (10.0)	
4	0 (0)	1 (2.5)	
Retinal break type, *n* (%)			0.75
Tear	15 (71.4)	27 (67.5)	
Hole	6 (28.6)	13 (32.5)	
Maximum retinal break location, *n* (%)			0.05
Upper	9 (42.9)	20 (50.0)	
Temporal	4 (19.0)	12 (30.0)	
Lower	8 (38.1)	4 (10.0)	
Nasal	0 (0)	4 (10.0)	
Retinal break size (h), *n* (%)			0.88
<1	17 (81.0)	33 (82.5)	
$\geqq 1$	4 (19.0)	7 (17.5)	
Combined scleral buckling, *n* (%)			0.003
Yes	5 (23.8)	40 (100.0)	
No	16 (76.2)	0 (0)	
Combined cataract surgery, *n* (%)			0.40
Yes	13 (61.9)	29 (72.5)	
No	8 (38.1)	11 (27.5)	
Surgical time, mean ± SD, min	126.4 ± 33.5	105.4 ± 29.7	0.01
ILM peeling, *n* (%)			0.23
Yes	7 (33.3)	6 (15.0)	
No	14 (66.7)	33 (82.5)	
Inverted flap	0 (0)	1 (2.5)	
Drainage retinotomy, *n* (%)			0.003
Yes	5 (23.8)	0 (0)	
No	16 (76.2)	40 (100.0)	
Tamponade agent, *n* (%)			0.02
Air	0 (0)	5 (12.5)	
SF6	15 (71.4)	33 (82.5)	
C3F8	2 (9.5)	1 (2.5)	
SO	4 (19.0)	1 (2.5)	

BCVA, best-corrected visual acuity; C3F8, perfluoropropane; ILM, internal limiting membrane; IOP, intraocular pressure; logMAR, logarithm of the minimum angle of resolution; SD, standard deviation; SF6, sulfur hexafluoride; SO, silicone oil.

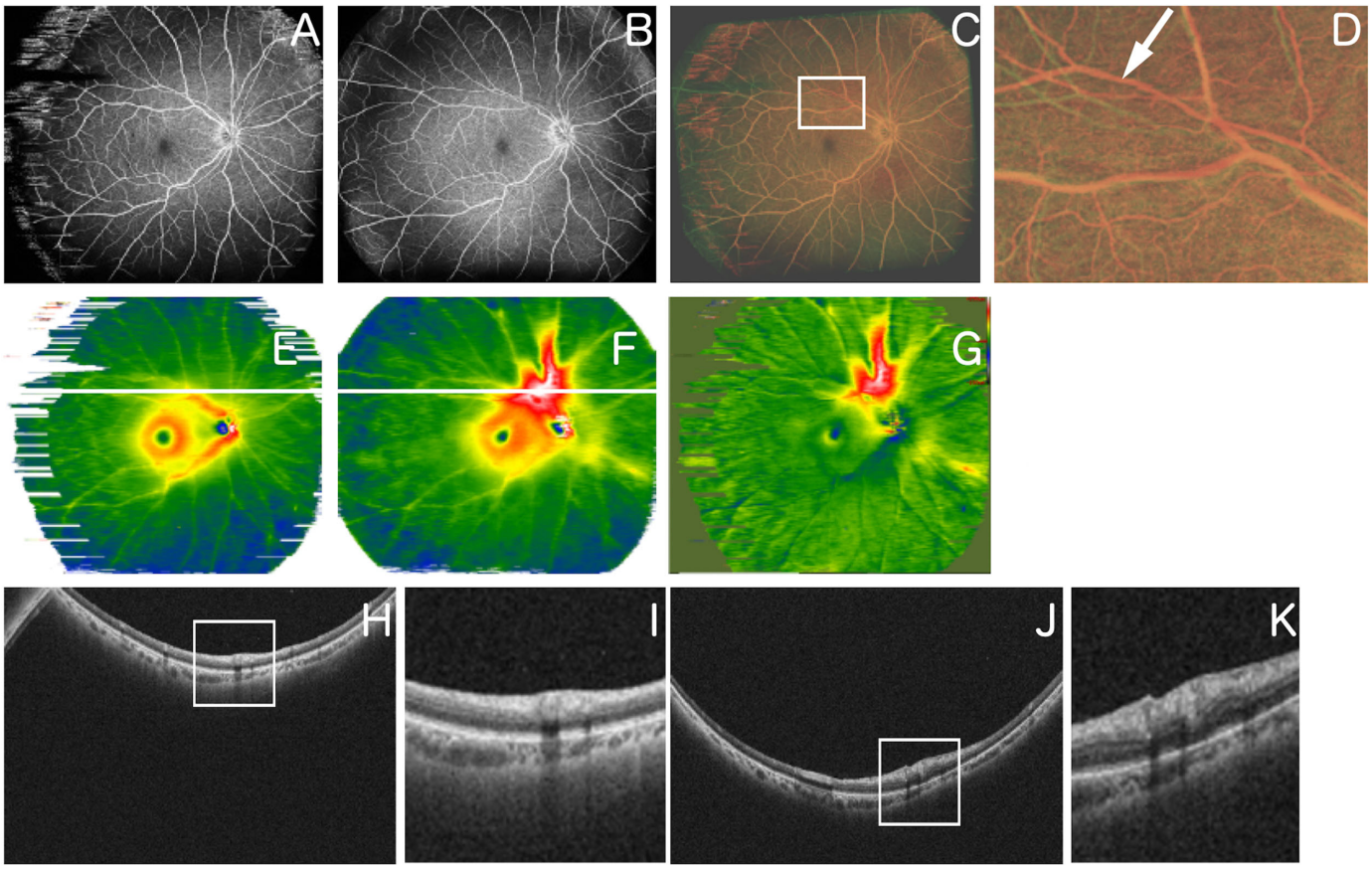

Figure 2. Representative case 1. A 59-year-old man underwent a vitrectomy for RRD. (**A**) An OCTA image obtained 1 month after surgery. (**B**) OCTA image obtained 2 months after surgery. (**C**) Overlaid image after changing **A** and **B** to *red* and *green*, respectively, and image processing. (**D**) Magnified image of the superior area **C** (area surrounded by *white squares*). The *white arrow* indicates retinal vessel tortuosity change. (**E**) Retinal thickness map image obtained 1 month after surgery. (**F**) Retinal thickness map image obtained 2 months after surgery. (**G**) An image obtained by comparing **E** and **F** using the OCT Research Tool, which can extract differences in retinal thickness. The area above the macula is displayed in a *warm color* in the retinal thickness map image and is thicker. (**H**) B-scan image of the part indicated by the *white line* in the image of **E**. (**I**) Magnified image of part of the image of **H** (area surrounded by a *white square*). (**J**) B-scan image of the part indicated by the *white line* in the image in **F**. (**K**) Magnified image of part of the image in **J** (area surrounded by a *white square*).

tortuosity changes were observed between 2 and 3 months postoperatively.

Retinal vessel tortuosity changes associated with alterations in subretinal fluid levels occurred only in cases after scleral buckling surgery, while proliferative membrane formations occurred after vitrectomy (including those with concomitant scleral buckling). To investigate relevant factors associated with proliferative membrane formation, we divided the 61 patients who underwent vitrectomy into two groups: those who developed proliferation (21 cases) and those who did not (40 cases).

Table 3 shows the comparison of the 11 baseline characteristics and six surgical procedures with or without proliferation. Among the 17 clinical factors analyzed, we observed nominal associations ($P < 0.05$) of 17 factors, including RD area ($P = 0.03$), maximum retinal break location ($P = 0.05$), combined scleral buckling ($P = 0.003$), surgical time ($P = 0.01$), intraoperative drainage retinotomy ($P = 0.003$), and tamponade agent ($P = 0.02$) with proliferation. In many cases, gas was used as a tamponade material during vitrectomy, leading to the presence of residual gas in the vitreous cavity during the initial 2 weeks postoperatively. However, in this study, gas, including perfluoropropane in the vitreous cavity, had dissipated by the 1-month postoperative stage. Among the five eyes in which silicone oil was used as the tamponade material, retinal vascular tortuosity changes due to proliferation were detected in four eyes. OCTA images were captured at the 2-week postoperative stage in two of these four eyes; additionally, retinal vascular tortuosity changes were detected between 2 weeks and 1 month postoperatively in these two eyes.

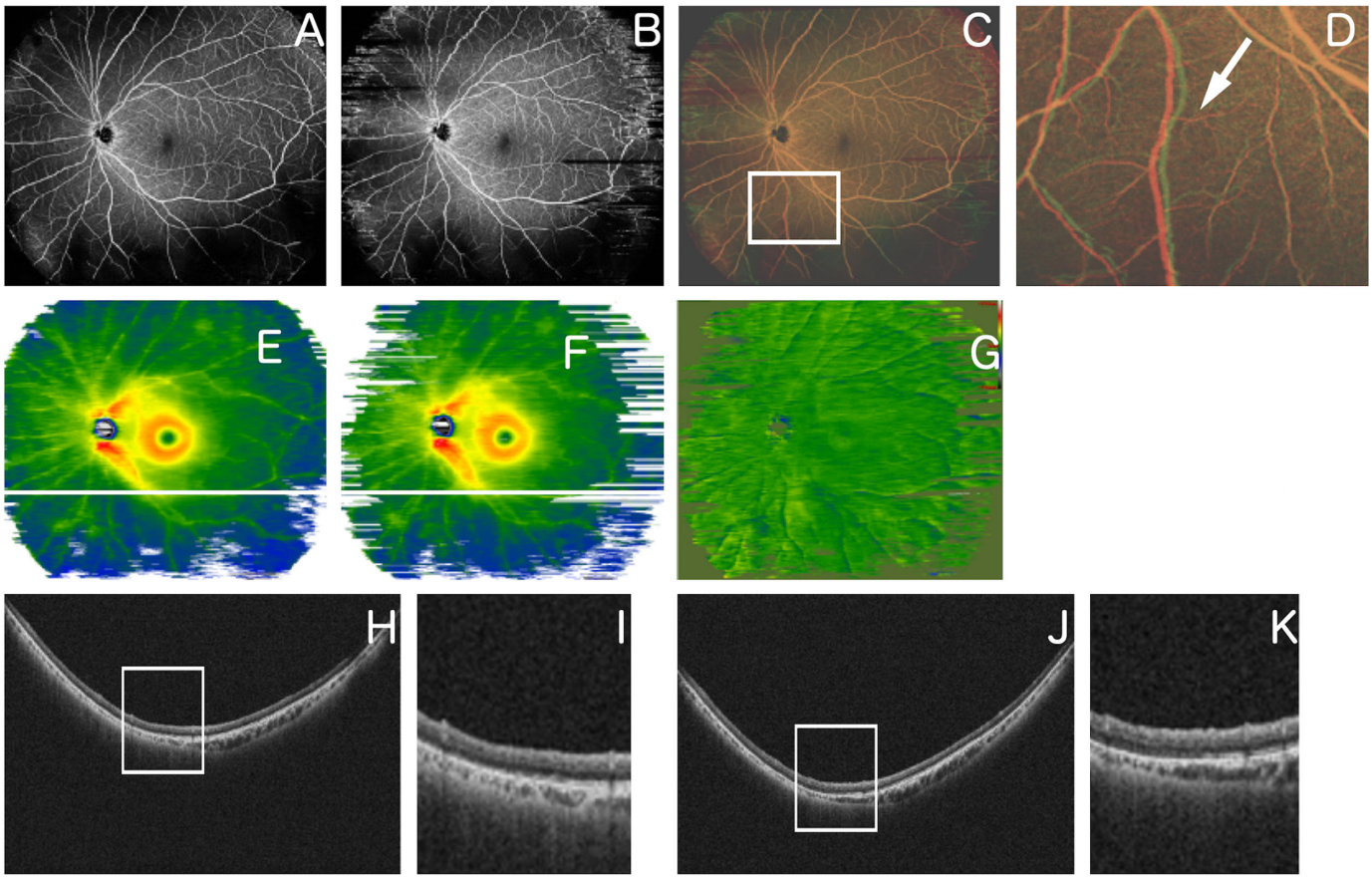

Figure 3. Representative case 2. A 51-year-old man underwent a vitrectomy for RRD. (**A**) An OCTA image obtained 1 month after surgery. (**B**) OCTA image obtained 2 months after surgery. (**C**) Overlaid image after changing **A** and **B** to *red* and *green*, respectively, and image processing. (**D**) Magnified image of the inferior area of **C** (area surrounded by a *white square*). The *white arrow* indicates retinal vessel tortuosity change. (**E**) Retinal thickness map image obtained 1 month after surgery. (**F**) Retinal thickness map image obtained 2 months after surgery. (**G**) Image obtained by comparing **E** and **F** using the OCT Research Tool, which can extract differences in retinal thickness; there is no *warm* or *cool color* on the image to indicate changes in retinal thickness. (**H**) B-scan image of the part indicated by the *white line* in the image of **E**. (**I**) Magnified image of part of the image of **H** (area surrounded by a *white square*). (**J**) B-scan image of the part indicated by the *white line* in the image in **F**. (**K**) Magnified image of part of the image in **J** (area surrounded by a *white square*).

Representative Cases

Case 1

A 59-year-old man underwent vitrectomy for RRD. Postoperative WF-OCTA images at 1 and 2 months following image processing revealed retinal vessel tortuosity changes in the superior optic disc region (Figs. 2A–D). Examination of the corresponding retinal thickness map indicated increased retinal thickness (Figs. 2E–G). B-scan images at the same location revealed progressive tissue proliferation over time (Figs. 2H–K). Hence, it is believed that retinal traction resulting from proliferative membrane development on the retinal surface led to retinal thickening and alterations in the retinal vascular patterns.

Case 2

A 59-year-old man underwent a vitrectomy for RRD. Overlapping WF-OCTA images acquired 1 and 2 months postoperatively revealed retinal vessel tortuosity changes in the inferior optic disc region (Figs. 3A–D). Examination of the corresponding retinal thickness map revealed minimal changes in thickness (Figs. 3E–G). B-scan images at the same location indicated slight proliferation on the retinal surface (Figs. 3H–K). In this case, retinal traction was attributed to subtle proliferative membranes on the retinal surface, although no significant changes in retinal thickness were observed. This case illustrates that while WF-OCTA detected alterations in the retinal status, such

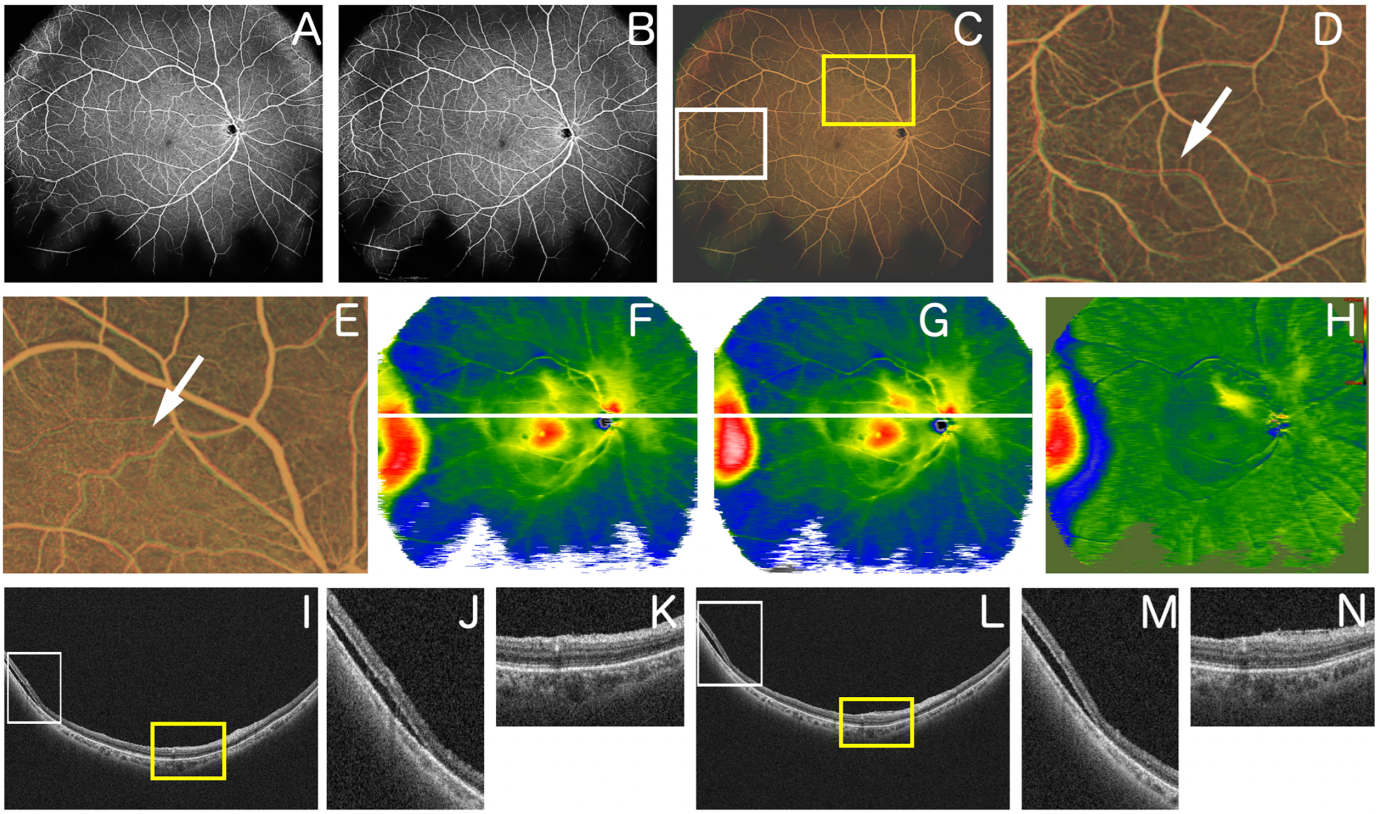

Figure 4. Representative case 3. A 67-year-old woman underwent a vitrectomy with scleral buckling for RRD. (**A**) OCTA image obtained 1 month after surgery. (**B**) OCTA image obtained 2 months after surgery. (**C**) Overlaid image after changing **A** and **B** to *red* and *green*, respectively, and image processing. (**D**) Magnified image of the inferior area of **C** (area surrounded by a *white square*). The *white arrow* indicates retinal vessel tortuosity change. (**E**) Magnified image of the inferior area of **C** (area surrounded by a *yellow square*). The *white arrow* indicates retinal vessel tortuosity change. (**F**) Retinal thickness map image obtained 1 month after surgery. (**G**) Retinal thickness map image obtained 2 months after surgery. (**H**) Image obtained by comparing **F** and **G** using the OCT Research Tool, which can extract differences in retinal thickness. The retinal thickness changes in the superior optic disc area, and the temporal area changes. (**I**) B-scan image of the part indicated by the *white line* in the image of **F**. (**J**) Magnified image of part of the image of **I** (area surrounded by a *white square*). (**K**) Magnified image of part of the image of **I** (area surrounded by a *yellow square*). (**L**) B-scan image of the part indicated by the *white line* in the image in **G**. (**M**) Magnified image of part of the image in **L** (area surrounded by a *white square*). (**N**) Magnified image of part of the image in **L** (area surrounded by a *yellow square*).

changes were not evident in the retinal thickness map image.

Case 3

A 67-year-old woman underwent a vitrectomy with scleral buckling for RRD. Overlapping WF-OCTA images acquired 1 and 2 months postoperatively revealed retinal vessel tortuosity changes in the superior optic disc and temporal regions (Figs. 4A–E). Examination of the corresponding retinal thickness map revealed retinal thickness changes (Figs. 4F–H). B-scan images at the superior optic disc region indicated progression of proliferation on the retinal surface, and B-scan images at the temporal region indicated movement of subretinal fluid (Figs. 4I–N). In this case, retinal traction resulting from proliferative membrane development on the retinal surface led to retinal thickening and retinal vessel tortuosity changes in the superior optic disc region. In the temporal region, both movement of subretinal fluid and retinal traction due to proliferative membrane led to retinal thickening and retinal vessel tortuosity changes.

Discussion

In this study, we used WF-OCT and WF-OCTA to assess the alterations in retinal vessel tortuosity and thickness in patients who underwent surgery for RRD. Our investigation of the origins of changes in retinal vessel tortuosity and alterations in retinal thickness revealed that most of these changes were attributed to the exacerbation of retinal traction caused

by proliferative membranes. This observation is consistent with prior studies that identified PVR as a prominent contributor to the recurrence of RD and the resulting retinal complications.

Furthermore, our study demonstrated that changes in retinal thickness were detectable in quadrants where changes in retinal vessel tortuosity were associated with fluctuations in subretinal fluid levels. However, in 7 of the 56 quadrants (12.5%) where changes were linked to intensified retinal traction from proliferative membranes, changes in retinal thickness were not apparent. This suggests an inconsistent correlation between retinal vessel tortuosity and retinal thickness in patients with RRD. Subretinal fluid level can affect retinal morphology in the vertical direction and the horizontal direction by changing retinal thickness and mound-like forms resulting in vessel tortuosity. Therefore, changes in the subretinal fluid could be identified in both the retinal thickness map and WF-OCTA images. Quadrants with subtle proliferative tissue on the retinal surface, which cause horizontal shifts, might not be discernible in retinal thickness maps. To identify subtle changes in retinal vessel tortuosity during PVR progression after RRD surgery, overlaying WF-OCTA images to assess vessel misalignment may be more beneficial than evaluating retinal thickness changes.

Despite several investigations to prevent of PVR, the current state of drug discovery remains insufficient.[13,19,20] Early detection of PVR symptoms may be pivotal when effective drugs for PVR prevention are available. Minor changes in retinal vessel tortuosity may signify early-stage PVR, as indicated by the previously mentioned PVR grading system.[14,21] Given the potential of PVR-suppressing treatments, our findings suggest that WF-OCTA and WF-OCT offer important insights into PVR diagnosis and management. Thus, it is considered highly valuable to have functionality integrated into OCT that enables the early detection of progression to PVR and automatically detects such changes. The ability to identify changes in retinal vessel tortuosity and retinal thickness enables clinicians to identify the underlying causes of retinal complications and tailor treatment strategies accordingly, especially if PVR-suppressing drugs become available; this will also be useful in explaining treatment plans to patients.

Factors associated with postoperative proliferation after vitrectomy include the location of preoperative retinal breaks, the extent of RD, and surgical procedures such as scleral buckling, tamponade agents, and surgical time. Previous reports have shown that the combination of scleral buckling and vitrectomy increases PVR risk compared to performing vitrectomy alone and that inferior breaks can pose a risk of recurrent detachment.[22,23] Taking these factors into account, it can be inferred that if the condition of RRD is severe, postoperative proliferative membranes are more likely to occur. Furthermore, the presence of drainage retinotomy was found to be related to proliferative membranes. This is consistent with previous reports showing that drainage retinotomy is involved in PVR and epiretinal membrane after RRD surgery.[24,25] Drainage retinotomy can be a risk for PVR because retinal pigment epithelial cells can invade the vitreous cavity through retinal tears and induce subsequent upregulation of profibrotic growth factors and inflammatory cytokines within the eye.[26] In this study, no new occurrences of retinal vessel tortuosity changes were observed between 2 and 3 months postoperatively. Considering this, it is conceivable that if postoperative proliferative membranes develop, they would likely commence proliferation between 1 and 2 months postoperatively at the latest. Further long-term follow-up may be necessary to understand how proliferative membranes proliferate and how they cease or regress.

Our results demonstrated that a significant proportion of quadrants displayed changes in retinal vessel tortuosity before image processing. However, upon application of the i2k Retina Pro software for processing, the number of detected retinal vessel tortuosity changes decreased notably. This highlights the importance of employing image-processing techniques to mitigate the influence of head misalignment and ocular rotation when scrutinizing WF-OCTA images. The software, renowned for its ability to automatically align and merge retinal images, offers a platform for comparing various modalities, such as fluorescein angiography and fundus photography, and is often employed to create seamless multi-image mosaics.[27] In our study, we harnessed the i2k Retina Pro for image registration, effectively rectifying the head and eye position discrepancies in WF-OCTA images. Although the algorithm is held by DualAlign as a trade secret, no differences were detected between the two images after image processing in healthy eyes. Moreover, in RRD eyes, morphologic changes were observed in B-scan images at all locations where retinal vessel tortuosity changes were detected in overlaid OCTA images. Fractal analysis can be used to recognize retinal vessels, and it may help detect retinal vessel tortuosity change. We used the i2k Retina Pro in this study,[28] and the comparison of the accuracy between our method and other techniques such as fractal analysis remains a future challenge. Given the precision achieved in both healthy and RRD eyes, this image-processing software has the potential to track temporal changes.

The limitations of our study include its retrospective design and relatively small sample size. Further

research with larger sample sizes and prospective study designs is imperative to validate these findings and to explore the potential clinical applications of WF-OCTA and WF-OCT in RRD management. We included only cases where clear OCTA images could be obtained at both 1 month and 2 months postoperatively. This implies that we excluded cases requiring reoperation within 2 months after surgery, cases where follow-up was interrupted within 2 months after surgery, and cases where OCTA imaging could not be obtained due to poor visual acuity. Another constraint of our study was the limited field of view in OCT imaging, especially for peripheral visualization. Understanding changes in the periphery, including the posterior edge of the scleral buckles, is crucial. However, owing to the limited field of view of WF-OCT obtained from the patient's frontal perspective in this study, our evaluation of the periphery was insufficient. Recognizing this limitation underscores the importance of future investigations employing imaging modalities that offer an expanded field of view. Furthermore, the detailed algorithm of i2k Retina Pro is unknown, raising the possibility of overestimation or underestimation of retinal vessel tortuosity changes after image processing. However, we also observed changes in retinal thickness and believe that significant changes were not overlooked.

In summary, our study provides valuable insights into the utility of WF-OCTA and WF-OCT for assessing changes in retinal vessel tortuosity and retinal thickness in patients with RRD. These imaging techniques provide a valuable means of identifying the roots of retinal complications and offer pertinent information for clinical management.

Acknowledgments

The authors thank Editage (www.editage.com) for English language editing.

Supported by Grants-in-Aid for Scientific Research from KAKENHI, #JP23K09046 (KI); the Eye Research Foundation for the Aged (KI); the Takeda Science Foundation (KI); the Bayer Retina Award Foundation (KI); the ROHTO Award (KI); Hoya Co. Ltd. (KHS); and Santen Pharmaceutical Co. Ltd. (KHS). The sponsor or funding organization had no role in the design or conduct of this research.

All data generated or analyzed during this study are included in this article. Further inquiries can be directed to the corresponding author.

Disclosure: **Y. Fukuda**, None; **K. Ishikawa**, None; **K. Kiyohara**, None; **Y. Maehara**, None; **R. Ji**, None; **K. Mori**, None; **Y. Kobayashi**, None; **M. Akiyama**, None; **T. Nakama**, None; **S. Notomi**, None; **S. Shiose**, None; **A. Takeda**, None; **K.-H. Sonoda**, None

References

1. Kunikata H, Aizawa N, Sato R, et al. Successful surgical outcomes after 23-, 25- and 27-gauge vitrectomy without scleral encircling for giant retinal tear. *Jpn J Ophthalmol*. 2020;64:506–515.
2. Adelman RA, Parnes AJ, Sipperley JO, Ducournau D. Strategy for the management of complex retinal detachments: the European Vitreo-Retinal Society Retinal Detachment Study Report 2. *Ophthalmology*. 2013;120:1809–1813.
3. Mitry D, Charteris DG, Yorston D, et al. The epidemiology and socioeconomic associations of retinal detachment in Scotland: a two-year prospective population-based study. *Invest Ophthalmol Vis Sci*. 2010;51:4963–4968.
4. Lin JB, Narayanan R, Philippakis E, Yonekawa Y, Apte RS. Retinal detachment. *Nat Rev Dis Primers*. 2024;10:18.
5. McCullough P, Mohite A, Virgili G, Lois N. Outcomes and complications of pars plana vitrectomy for tractional retinal detachment in people with diabetes: a systematic review and meta-analysis. *JAMA Ophthalmol*. 2023;141:186–195.
6. Yorston D, Donachie PHJ, Laidlaw DA, et al. Stratifying the risk of re-detachment: variables associated with outcome of vitrectomy for rhegmatogenous retinal detachment in a large UK cohort study. *Eye (Lond)*. 2023;37:1527–1537.
7. Ong SS, Ahmed I, Gonzales A, et al. Management of uncomplicated rhegmatogenous retinal detachments: a comparison of practice patterns and clinical outcomes in a real-world setting. *Eye (Lond)*. 2023;37:684–691.
8. Obata S, Sawada O, Kakinoki M, et al. Effects of internal limiting membrane peeling on anatomical and functional outcomes in macula-off rhegmatogenous retinal detachment complicated by proliferative vitreoretinopathy: Japan-Retinal Detachment Registry. *Jpn J Ophthalmol*. 2023;67:417–423.
9. Ozsaygili C, Bayram N. Effects of different tamponade materials on macular segmentation after retinal detachment repair. *Jpn J Ophthalmol*. 2021;65:227–236.

10. Ahmadieh H, Feghhi M, Tabatabaei H, et al. Triamcinolone acetonide in silicone-filled eyes as adjunctive treatment for proliferative vitreoretinopathy: a randomized clinical trial. *Ophthalmology*. 2008;115:1938–1943.
11. Mudhar HS. A brief review of the histopathology of proliferative vitreoretinopathy (PVR). *Eye (Lond)*. 2020;34:246–250.
12. Ishikawa K, Yoshida S, Nakao S, et al. Periostin promotes the generation of fibrous membranes in proliferative vitreoretinopathy. *Faseb J*. 2014;28:131–142.
13. Wu F, Eliott D. Molecular targets for proliferative vitreoretinopathy. *Semin Ophthalmol*. 2021;36:218–223.
14. Machemer R, Aaberg TM, Freeman HM, et al. An updated classification of retinal detachment with proliferative vitreoretinopathy. *Am J Ophthalmol*. 1991;112:159–165.
15. Manjunath V, Papastavrou V, Steel DH, et al. Wide-field imaging and OCT vs clinical evaluation of patients referred from diabetic retinopathy screening. *Eye (Lond)*. 2015;29:416–423.
16. Poddar R, Migacz JV, Schwartz DM, Werner JS, Gorczynska I. Challenges and advantages in wide-field optical coherence tomography angiography imaging of the human retinal and choroidal vasculature at 1.7-MHz A-scan rate. *J Biomed Opt*. 2017;22:1–14.
17. Elnahry AG, Ramsey DJ. Automated image alignment for comparing microvascular changes detected by fluorescein angiography and optical coherence tomography angiography in diabetic retinopathy. *Semin Ophthalmol*. 2021;36:757–764.
18. Ge R, Fang Z, Wei P, et al. UWAFA-GAN: ultra-wide-angle fluorescein angiography transformation via multi-scale generation and registration enhancement. *IEEE J Biomed Health Inform*. 2024:1–10.
19. Pennock S, Haddock LJ, Eliott D, Mukai S, Kazlauskas A. Is neutralizing vitreal growth factors a viable strategy to prevent proliferative vitreoretinopathy? *Prog Retin Eye Res*. 2014;40:16–34.
20. Kita T, Hata Y, Arita R, et al. Role of TGF-beta in proliferative vitreoretinal diseases and ROCK as a therapeutic target. *Proc Natl Acad Sci USA*. 2008;105:17504–17509.
21. The classification of retinal detachment with proliferative vitreoretinopathy. *Ophthalmology*. 1983;90:121–125.
22. Salabati M, Massenzio E, Kim J, et al. Primary retinal detachment repair in eyes deemed high risk for proliferative vitreoretinopathy: surgical outcomes in 389 eyes. *Ophthalmol Retina*. 2023;7:954–958.
23. Williamson TH, Lee EJ, Shunmugam M. Characteristics of rhegmatogenous retinal detachment and their relationship to success rates of surgery. *Retina*. 2014;34:1421–1427.
24. Ohara H, Yuasa Y, Harada Y, et al. Drainage retinotomy is a risk factor for surgical failure after pars plana vitrectomy in patients with primary uncomplicated rhegmatogenous retinal detachment. *Retina*. 2022;42:2307–2314.
25. Ishikawa K, Akiyama M, Mori K, et al. Drainage retinotomy confers risk of epiretinal membrane formation after vitrectomy for rhegmatogenous retinal detachment repair. *Am J Ophthalmol*. 2022;234:20–27.
26. Pastor JC, Rojas J, Pastor-Idoate S, et al. Proliferative vitreoretinopathy: a new concept of disease pathogenesis and practical consequences. *Prog Retin Eye Res*. 2016;51:125–155.
27. Chen J, Ausayakhun S, Ausayakhun S, et al. Comparison of autophotomontage software programs in eyes with CMV retinitis. *Invest Ophthalmol Vis Sci*. 2011;52:9339–9344.
28. Magesan K, Gnanaraj R, Tojjar J, et al. Fractal analysis of the macular region in healthy eyes using swept-source optical coherence tomography angiography. *Graefes Arch Clin Exp Ophthalmol*. 2023;261:2787–2794.